Turkish Journal of Electrical Engineering & Computer Sciences

http://journals.tubitak.gov.tr/elektrik/

Research Article

Turk J Elec Eng & Comp Sci
(2017) 25: 4474 – 4485

doi:10.3906/elk-1702-295

Koch fractal-based hexagonal patch antenna for circular polarization

Manisha GUPTA[1,*], **Vinita MATHUR**[2]
[1]Department of Physics, JECRC University, Jaipur, India
[2]Department of Electronics and Communication, JECRC University, Jaipur, India

Received: 21.02.2017 • **Accepted/Published Online:** 24.08.2017 • **Final Version:** 03.12.2017

Abstract: The design and performance of an inset feed modified hexagonal patch antenna for possible applications in ultrawideband communication systems is reported. The inset feed hexagonal patch antenna is modified by introducing a fractal up to the second iteration. A right-angled isosceles triangular microstrip antenna is used in the Koch fractal structure on the edges. The proposed antenna is a combination of two standard fractal structures, i.e. Sierpinski and Koch. A rectangular defect in the ground has also been done. The antenna is simulated by applying CST Microwave Studio simulation software. The results are verified by fabricating the antenna and tested using a vector network analyzer. The developed design shows good matching with the feed network at frequencies of 3.1 GHz, 6.9 GHz, 7.3 GHz, 8.5 GHz, and 9.1 GHz. The simulated peak gain of the antenna at resonant frequencies is 4.08 dB, 4.79 dB, 3.85 dB, 3.46 dB, and 3.01 dB. The antenna is fabricated on FR-4 substrate having size 30 $\times$ 35 $\times$ 1.59 mm^3. It covers the S and X band range. It can be used for microwave applications as it is a part of the microwave spectrum, for wireless networking devices coming under IEEE standards. It can also be used for multimedia applications like mobile TV and satellite radio that use the S band as their frequency range and in home-based consumer electronics like microwave ovens, cordless phones, and wireless headphones. For higher ranges, i.e. in the X band, it can be used in radars, satellites, and military appliances.

Key words: Microstrip patch antenna, ultrawideband, Koch fractal, defected ground structure, circular polarization

1. Introduction

In the field of portable systems, there has been immense improvement due to the advancement of microstrip patch antennas. Various applications at divergent frequency bands are sustained by these systems. Hence, there is a need for an antenna that is multiband, circularly polarized, and small in size. Multiband, lower weight, wide bandwidth, smaller dimensions, and cheap in cost are some of the requirements that can be achieved by using fractal-shaped antennas rather than conventional ones. This has initiated research about antennas in various directions, and it is found that the following designs are particularly focused on the generation of self-similar shapes that generate multifrequency, which results in increased bandwidth and size reduction of the antenna and has better characteristics when compared with conventional microstrip antennas. Examples of these mathematical structures are the von Koch snowflake, Sierpinski carpet, Mandelbrot set, Lorentz attractor, and Minkowski curve [1–6]. Another requirement of the antenna is circular polarization (CP), which has obtained consideration because of the enormous number of appliances used in military, wireless communication, and global navigation satellite systems. Positioning of the electric field at the receiver and transmitter is not enforced for

*Correspondence: drguptamanisha@gmail.com

a circularly polarized antenna. Miniaturization, a less complex structure, and less RF power loss are some of the advantages that are achieved by using CP.

There are different approaches possible in the literature to achieve a CP microstrip antenna, such as a square slot with modified edges [7] or modified edges of a U-shaped tuning stub [8]. By introducing a defect in the ground, using different metastructures or resonators disturbs the properties of the aerial for producing CP radiation [9,10]. Orthogonal feeds, single feeds, and altered structures are some of the techniques that can be used to achieve CP in a single patch [11,12]. Antenna dimensions and wavelength have a strong relation. Radiation resistance, gain, and bandwidth values decrease if the transmitter size is less than $\lambda/2$, and because of this factor, the efficiency reduces. One of the effects of a defected ground structure (DGS) is to reduce the size of the antenna and coupling in arrays [13,14]. To reduce complexity and make the structure simple, multiband aerial is required. H-shape, U-shape, and hexagonal slots with slits have been used to implement triple-band antennas [15,16]. Many papers based on hexagonal patches with fractal geometry have been published, including the following:

1. Analysis of mushroom-type electromagnetic bandgap structure using fractal geometry on a hexagonal patch antenna [17].
2. Hexagonal fractal multiband antenna for UWB [18–20] and with DGS [21,22].
3. Hexagonal patch with a combination of Koch [23,24] and trapezoidal elements added on the edges [25].

A microstrip-fed hexagonally shaped aerial for UWB application is proposed in this paper. The patch is fractured once and on the edges of the fractured patch a Koch snowflake is implemented. The proposed antenna is a combination of two standard fractal structures, i.e. Sierpinski and Koch. A rectangular defect in the ground has also been done. The patch shape selected is hexagonal because it resembles a circular shape, which is capable of accomplishing circular polarization. Further, a comparison is done in terms of antenna parameters such as return loss, bandwidth, and gain. The objective of the paper is to design a circularly polarized fractal microstrip antenna structure over the UWB frequency range with better gain, VSWR, and bandwidth. As shown in the Table, a comparison with other references has been done. Most of the papers use dual or triple resonant frequency, for which the size is equally high. For our proposed antenna, we get four bands with comparably reduced size.

Table. Comparison of the proposed antenna with reference antennas.

S. no.	Reference	Size (mm × mm, W × L)	Resonant frequencies
1	Ref. [26]	100 × 100	4.71–6 GHz
2	Ref. [27]	100 × 60	2.4–2.7 GHz, 3.4–3.7 GHz, 5.2–5.8 GHz
3	Ref. [28]	100 × 45	1.82–2.19 GHz, 4.95–5.31 GHz
4	Ref. [8]	90 × 90	3.1–12 GHz
5	Ref. [7]	70 × 70	2.7–4.3, 4.3–5.1 GHz
6	Ref. [2]	70 × 95	1.45–1.61, 2.4–2.63 GHz
7	Ref. [29]	59 × 90	2.17, 4.47, 5.6 GHz
8	Ref. [30]	54 × 75.8	2.4 GHZ, 7.4 GHz, 9.2 GHz
9	Ref. [31]	53.37 × 75.20	1.74, 3.85, 5.05 GHz
10	Ref. [11]	40.7 × 40.7	3.1, 4.2, 5 GHz
11	Proposed antenna	30 × 35	3.1, 6.9, 8.4, 9.1 GHz

2. Antenna design

This section describes the antenna geometry and the design process. Analysis of the proposed structure is obtained by using CST Microwave Studio. A circular patch antenna is taken as a base for designing the hexagonal patch as the shapes are in close relation to each other.

The resonant frequency for the lowest order mode may be approximately calculated from:

$$kS = 2.01, \tag{1}$$

where S is the side of a hexagon. In the derivation of the above relationship, the hexagonal element is assumed to be a resonant cavity with perfectly conducting side walls. A circular disk is a limiting case of a polygon with a large number of sides; the resonant frequency for the dominant as well as for the higher order modes may be calculated from Eq. (2):

$$f_r = \frac{k_{nm}\, c}{2\pi a_e \sqrt{\varepsilon_r}}, \tag{2}$$

where $k_{nm} = ka$ is the mth zero of the derivative of the Bessel function of order $n$and $c$is the velocity of light in free space. An effective radius a_e has been introduced in the equation to account for the fringe fields along the edge of the resonator:

$$a_e = a\left[1 + \frac{2h}{\pi a \varepsilon_r}\left(\ln\frac{\pi a}{2h} + 1.7726\right)\right]^{1/2}, \tag{3}$$

replacing a by the equivalent a_{eq}. The equivalent radius a_{eq} is determined by comparing areas of a hexagon and a circular disk of radius a_{eq}:

$$\pi a_{eq}^2 = \frac{3\sqrt{3}\, S^2}{2}, \tag{4}$$

or

$$a_{eq} = 0.9094S. \tag{5}$$

Thus, the resonant frequency of a hexagonal element may be written as:

$$f_r = \frac{K_{nm}\, c}{2\pi(0.9094\, S)\sqrt{\varepsilon}_r} = \frac{1.1K_{nm}\, c}{2\pi\, S\sqrt{\varepsilon}_r}, \tag{6}$$

where K_{nm} has been defined as follows:

Mode (n,m)	Root ka
0,1	0
1,1	1.84118
2,1	3.05424
0,2	3.83171
3,1	4.20119

Putting these values in the equation at resonant frequency f_r = 4 GHz.

Radius of patch = 11.5 mm.

Values of the antenna used are: FR-4 epoxy substrate (ε_r = 4.4), thickness h = 1.59 mm, and loss tangent tan δ = 0.0024. As we have this material available, the antenna is fabricated at 30 × 35 mm^2 in size.

The flowchart of the design process of the designed antenna is shown in Figure 1.

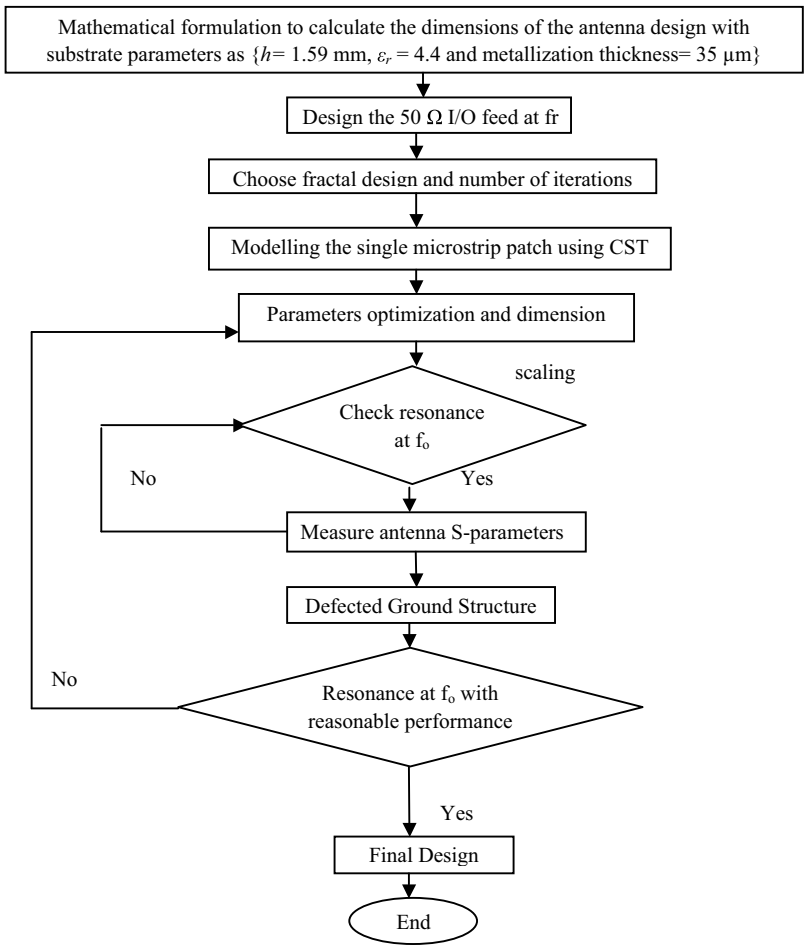

Figure 1. Flowchart of design process.

3. Results and parametric study

This section discusses the antenna with variations in its design parameters. The outcomes are obtained by simulating it with CST Microwave Studio. Return loss, gain, bandwidth, and radiation pattern are measured. The output criterion of the designed antenna is considered by modifying one design parameter at a time and adjusting the others.

3.1. Effect of varying inset width

The feed selected is inset feed for this patch because the input impedance of the aerial can be controlled by altering the length of feed and width of the inset feed. Return loss improves when proper matching is done. Figure 2 shows the variation in width of inset feed. These design parameters are obtained after extensive optimizations to give optimum results. However, as seen from the figure, better S_{11} values are obtained by fixing the width to 6 mm.

3.2. Effect of varying feed width

The reflected power and loss of signal is much lower when proper matching is done, i.e. at W_feed = 3 mm as observed in Figure 3. The considered feed line is electrically thick and contributes in the overall performance of antenna.

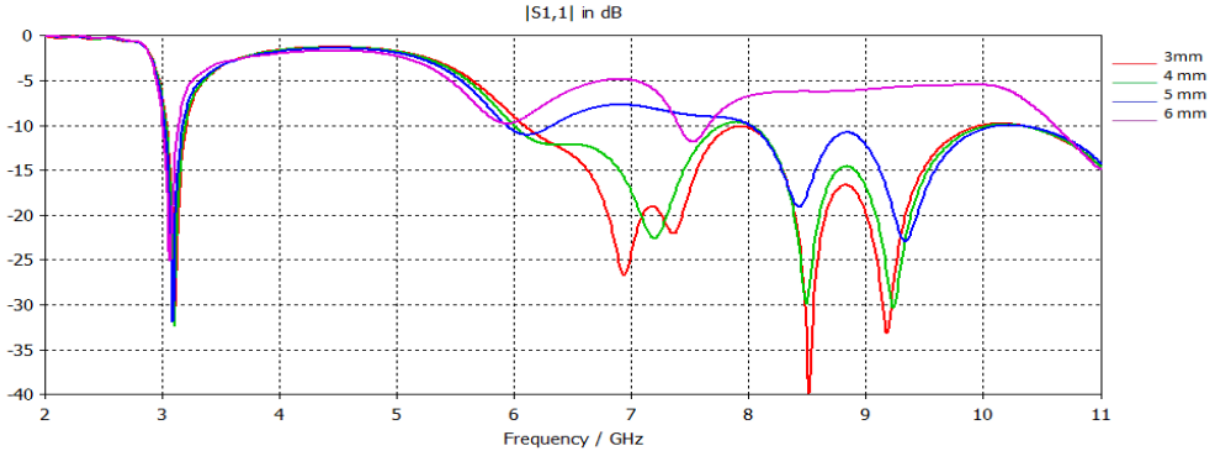

Figure 2. Comparison of S_{11} with variation in inset feed.

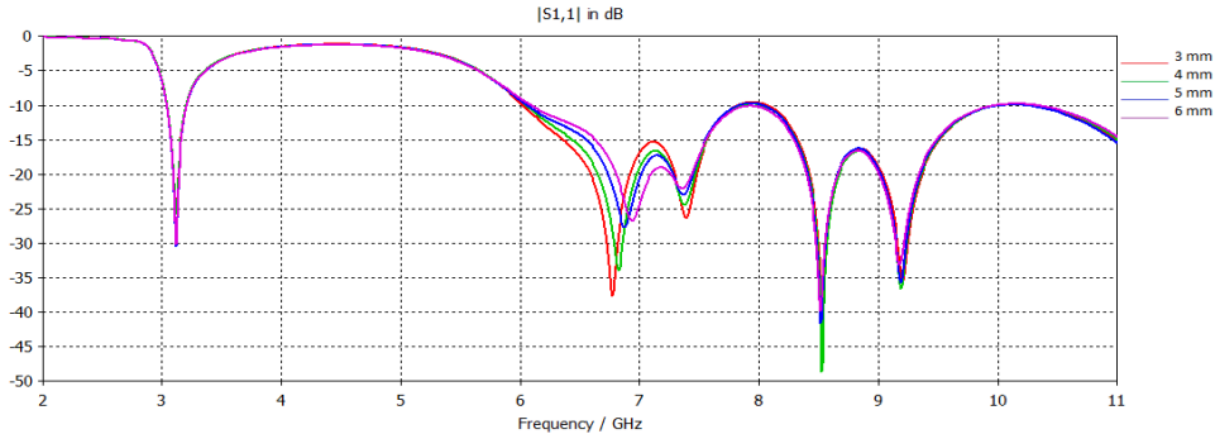

Figure 3. Comparison of S_{11} with variation in feed width.

3.3. Effect of varying ground dimensions (x)

The dimensions of the defected ground plane are varied and the consequence of this variation on the return loss of the patch antenna is observed. The resonance frequencies and the simulated impedance bandwidths for the different dimensions of ground are shown in Figure 4. The impedance bandwidth could be further enhanced by applying different sizes of ground plane lengths. For this, variations in ground dimensions (x) were done, as shown in Figure 4. Better results are observed by keeping the dimensions of the defected ground as 29.4 $\times$ 12 mm^2 (W $\times$ L). Multiband results are observed in this case.

3.4. Effect of fracturing the patch

In the first step of modification, the patch is fractured. First a hexagon patch is removed such that the center point of both the hexagons coincides with a radius of 4 mm and then on its edges a Koch snowflake is added, as shown in Figure 5. Fracturing is particularly focused on generation of multifrequency, which results in increased bandwidth and size reduction of the antenna and has better characteristics when compared with conventional microstrip antennas. They show multiband characteristics because of their self-similar properties.

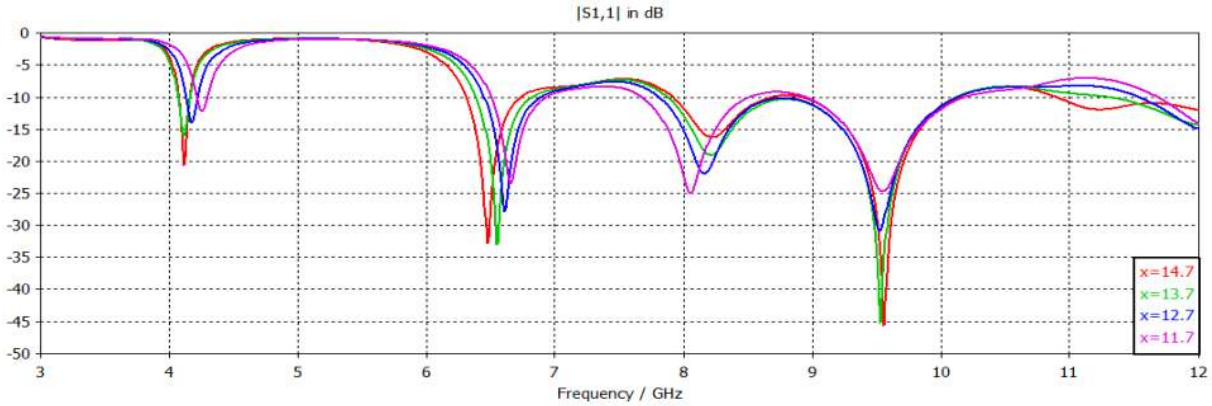

Figure 4. Comparison of S_{11} with variation in defect of ground.

The iterative function system (IFS) algorithm is applied to generate the succession of curves that converge to the ideal fractal shape. These IFSs are used to construct certain fractals. It can be proved that the starting element is irrelevant to converge to the fractal shape; however, when analyzing the fractal antenna behavior, it is especially interesting to compare it with that of the closest Euclidean version, i.e. a straight monopole. Such a straight monopole is referred to as K0 (the zeroth iteration of the fractal construction), while the remaining objects of the iterations will be referred to as K1, K2, ..., K_n. The next iteration, K1, is obtained by applying the four similarity transformations to K0. Figure 6 shows the fabricated antenna structure.

Simulated impedance bandwidth (VSWR $<$ 2) is 5.17% and 49.9% and measured values are 6.47%, 17.81%, and 21.91% as obtained using a vector network analyzer. The differences between these results are due to the following factors: variation of the characteristic parameters of the selected medium material, i.e. substrate thickness, soldering effects, and the quality of the SMA connector used. Figure 7 shows the measured and simulated comparison S_{11} graph of the final fractured DGS hexagonal structure.

The axial ratio value measures circular polarization. Values of axial ratio less than 3 dB over the frequency band make the aerial circularly polarized in that frequency band. A graph of the axial ratio of the final structure is depicted in Figure 8.

Surface current distribution of the aerial at resonating frequencies is depicted in Figure 9. Due to the fracture in the patch, the path of the current is distributed and the path of the current is increased, leading to enhanced values as compared to the normal patch. Increase in surface current path results in miniaturization. The current is mainly concentrated in the interior of the patch around the Koch snowflake. At the lower resonant frequency, the current is mainly concentrated at the edges of the outer patch, but as the frequency increases, the concentration of the current is more towards the inner fractured patch along with the feed line.

VSWR is a measure that describes the matching of impedance in the antenna to the connecting line it is associated to. Voltage along the transmission line determines the VSWR. At resonant frequencies, the value is approximately between 1 and 2, as shown in Figure 10. Figure 11 shows the radiation pattern at resonant frequencies.

With a defect in the ground, resonant frequency is added at lower frequency values. Gain obtained in this case is 3.38 dB, 6.64 dB, 3.12 dB, and 4.28 dB.

At the receiver side, nearly constant group delay should be there in the UWB range for efficient working of the antenna. The group delay is shown in Figure 12. It is the derivative of the far-field phase with respect to the frequency. A straight graph is obtained for almost the entire frequency range. The simulated group delay

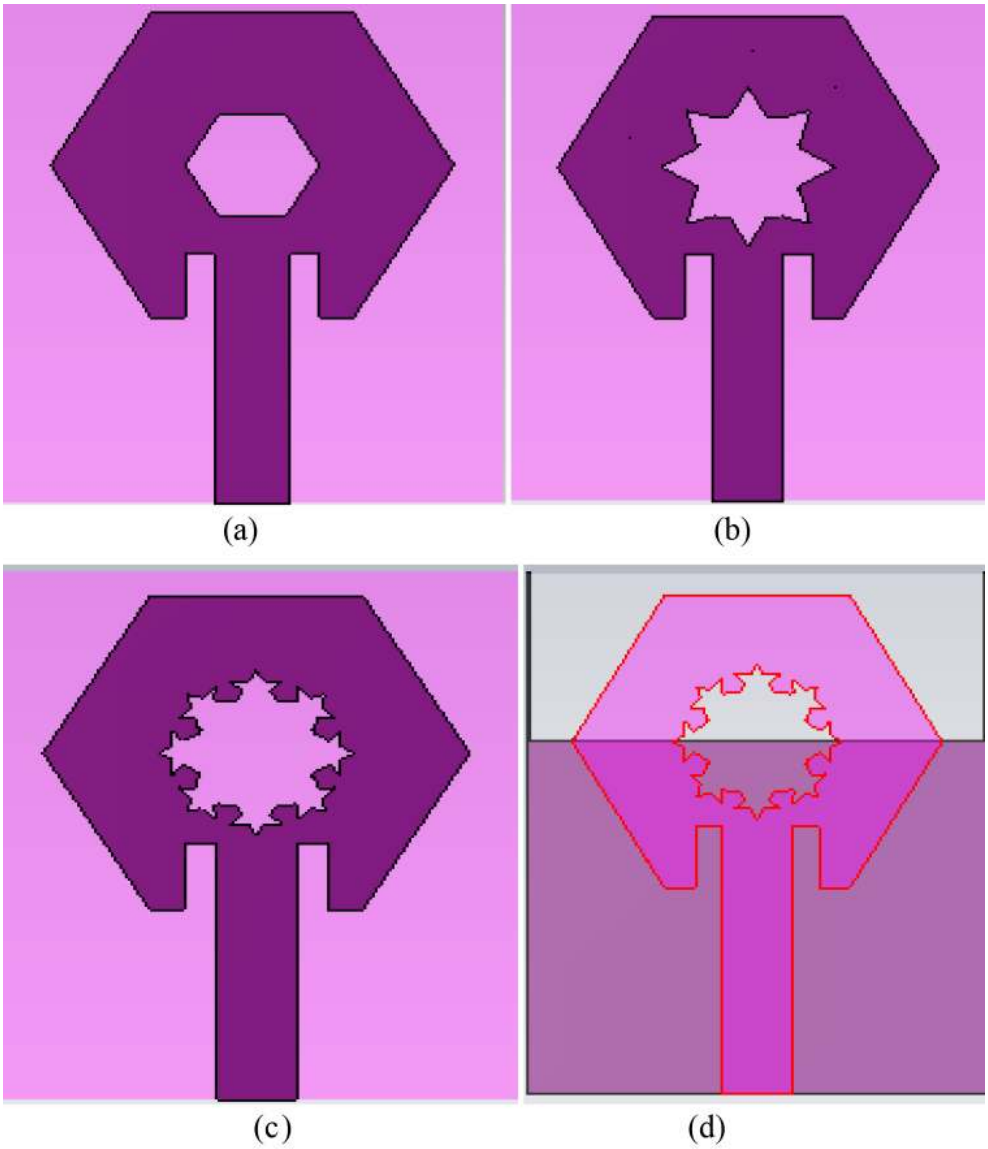

Figure 5. a) Geometry of fractal hexagonal structure, b) structure with Koch fractal, c) structure with first iteration Koch fractal, d) structure with ground and fractal shape.

remains almost unchanged in the desired frequency and this indicates a good performance in time. Linear phase response is required to efficiently utilize the UWB range. As seen in Figure 13, there is phase surface excitation due to the linear phase and less distortion in the signal transmission.

4. Conclusion

This is the first time that a right-angled isosceles triangular microstrip antenna has been used in a Koch fractal structure. The proposed antenna is a combination of two standard fractal structures, i.e. Minkowski and Koch. A rectangular defect in the ground has also been done. In this structure, both the ground plane and the radiating patch are modified to obtain the desired performance. The Koch snowflake fractal and defected ground structure arrangement has been designed on a glass epoxy FR-4 substrate. The designed antenna presents much improved

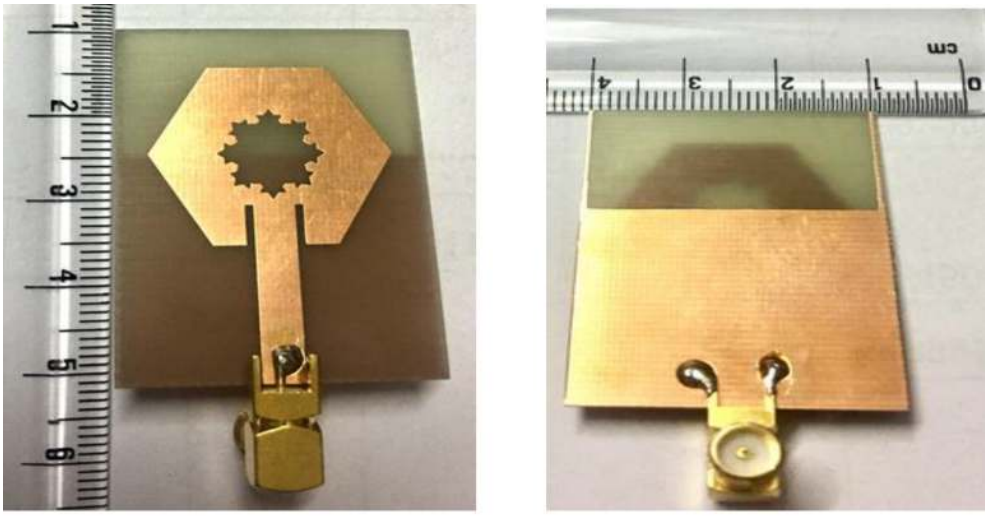

Figure 6. a) Front view, b) back view.

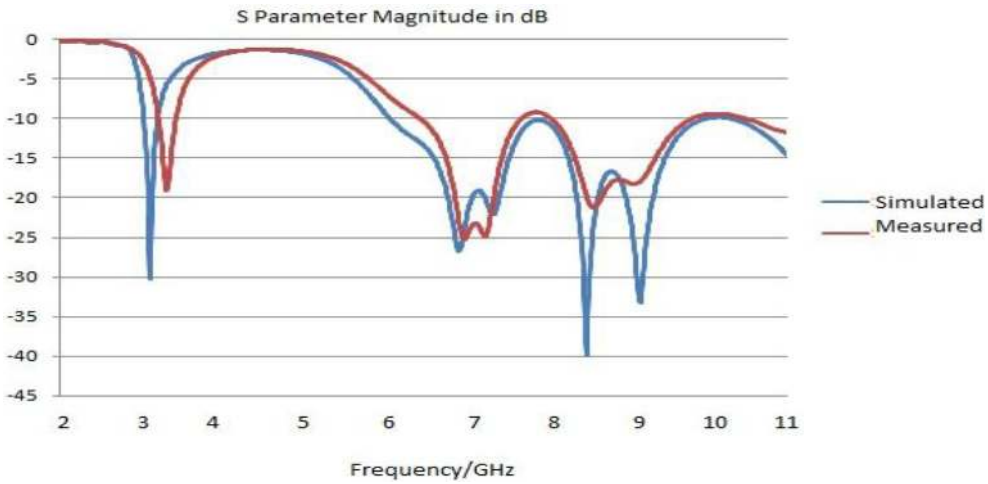

Figure 7. Comparison between simulated and measured values of S_{11}.

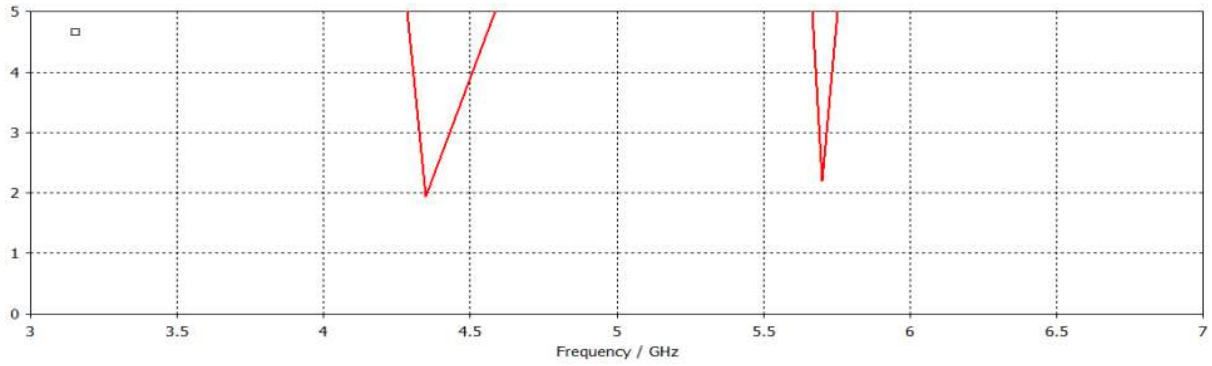

Figure 8. Axial ratio graph.

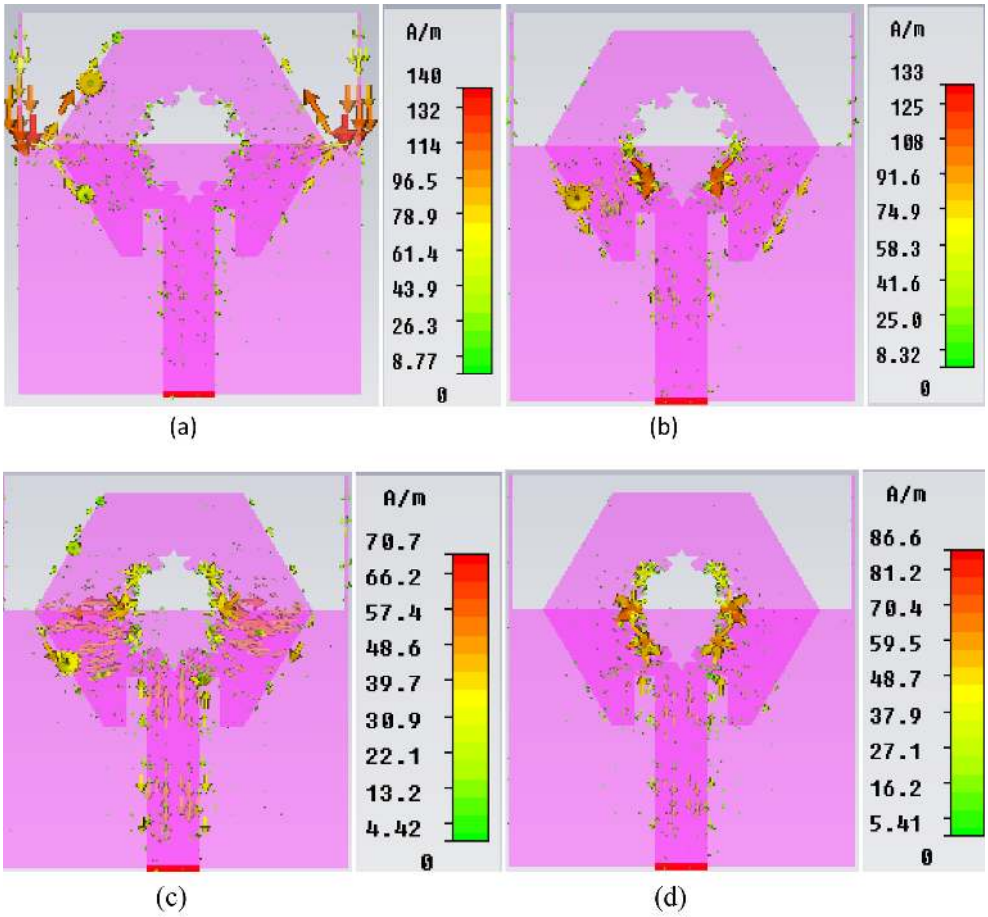

Figure 9. Surface current density of patch antenna at resonant frequencies: a) 3.1 GHz, b) 6.9 GHz, c) 8.4 GHz, d) 9.1 GHz.

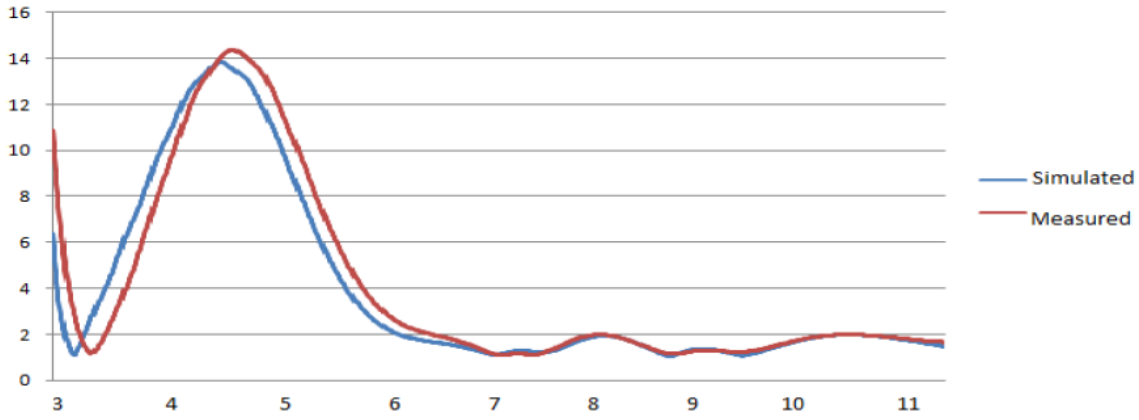

Figure 10. VSWR of the proposed structure.

gain and axial ratio. These improved parameters are achieved without much increase in the thickness of the structure. In several modern wireless and satellite communication systems, multiband along with circularly polarized radiations with higher axial ratio bandwidth are desired, and this antenna may prove to be a useful structure for these systems. Different characteristics of antennas such as return loss, radiation pattern, and

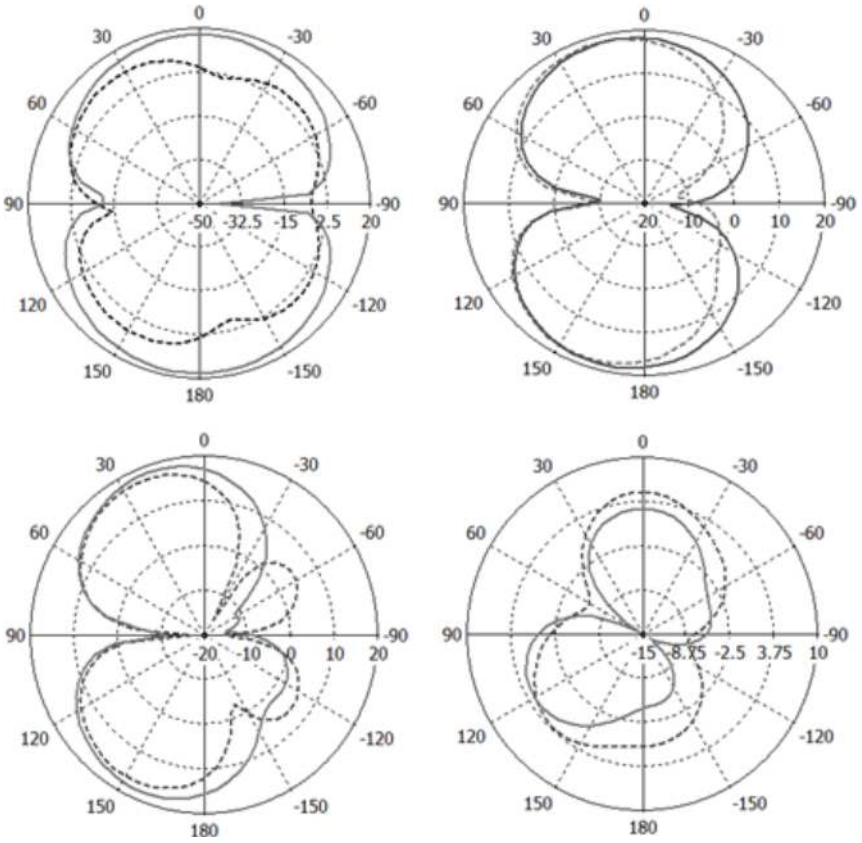

Figure 11. E-field patterns at various frequencies ($\varphi = 90^\circ$) (___ simulated, —- measured): a) 3.1 GHz, b) 6.9 GHz, c) 8.4 GHz, d) 9.1 GHz.

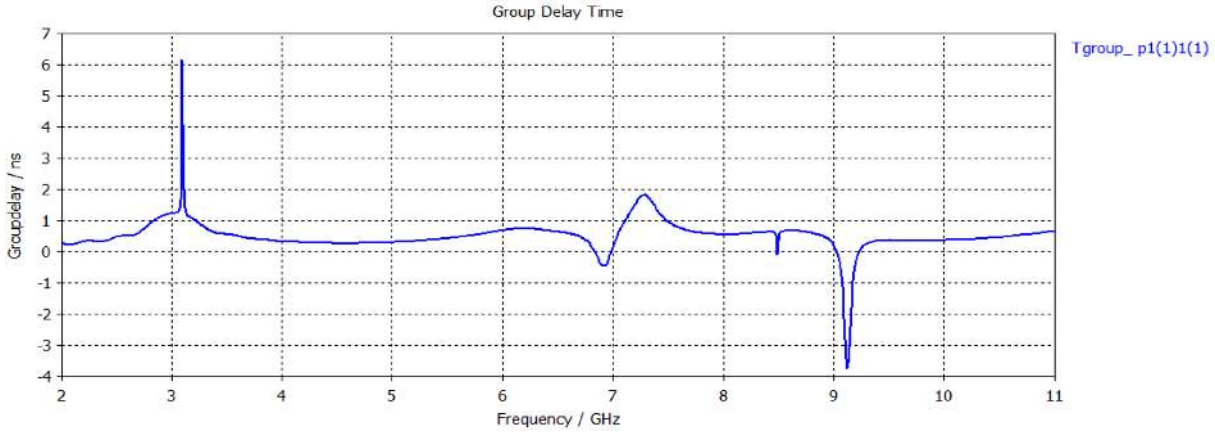

Figure 12. Group delay of the antenna.

gain are measured. It can be used for microwave applications as it is a part of the microwave spectrum, for wireless networking devices coming under IEEE standards. It can also be used for multimedia applications like mobile TV and satellite radio that use the S band as their frequency range, as well as in home-based consumer electronics like microwave ovens, cordless phones, and wireless headphones. For higher ranges, i.e. in the X band, it can be used in radars, satellites, and military appliances.

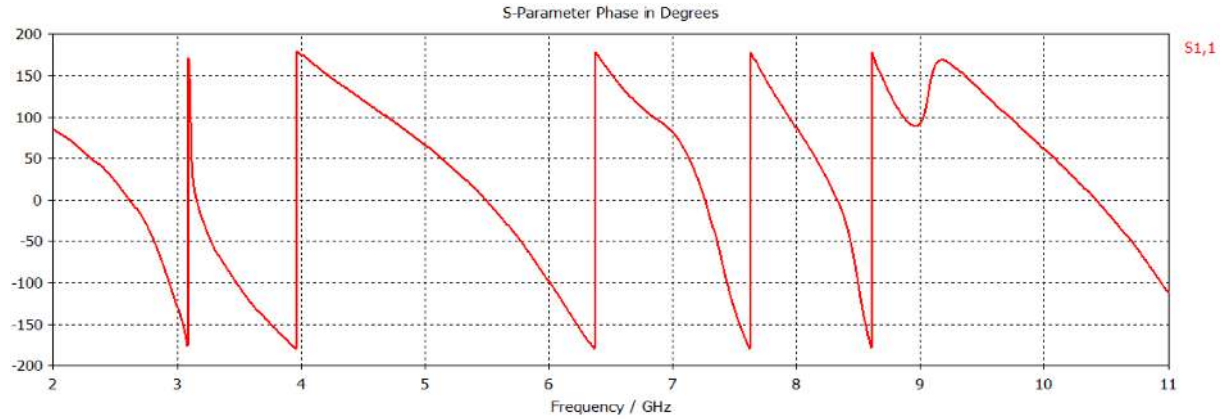

Figure 13. Phase plot of the proposed structure.

Acknowledgment

The authors would like to thank Professor Deepak Bhatnagar, University of Rajasthan, Jaipur, for providing us the measurement facilities in the lab.

References

[1] Husseini MA, Ramadan A, Tawk Y, Hajj AE, Kabalan KY. Design and ground plane optimization of a CPW-fed ultra-wideband antenna. Turk J Elec Eng & Comp Sci 2011; 19: 243-250.

[2] Srain SS, Sivia JS. Design of C shape modified Sierpinski carpet fractal antenna for wireless applications. In: IEEE 2016 Electrical, Electronics, and Optimization Techniques Conference; 3–5 March 2016; Chennai, India. New York, NY, USA: IEEE. pp. 821-824.

[3] Werner DH, Gangul S. An overview of fractal antenna engineering research. IEEE Antenn Propag M 2003; 45: 38-57.

[4] Li D, Mao JF. Coplanar waveguide-fed Koch-like sided Sierpinski hexagonal carpet multifractal monopole antenna. IET Microw Anten P 2014; 8: 358-366.

[5] Fallahi H, Atlasbaf Z. Bandwidth enhancement of a CPW-fed monopole antenna with small fractal elements. AEU-Int J Electron C 2015; 69: 590-595.

[6] Chawla P, Khanna R. A novel approach of design and analysis of fractal antenna using a neurocomputational method for reconfigurable RF MEMS antenna. Turk J Elec Eng & Comp Sci 2016; 24: 1265-1278.

[7] Oraizi H, Hedayati S. Circularly polarized multiband microstrip antenna using the square and Giuseppe Peano fractals. IEEE T Antenn Propag 2012; 60: 3466-3471.

[8] Dawood SJ, Salari MA, Ghoochani OH. Cross-slot antenna with U-shaped tuning stub for ultra-wideband applications. Int J Antenn Propag 2008; 2008: 262981.

[9] Dong Y, Toyao H, Itoh T. Compact circularly-polarized patch antenna loaded with metamaterial structures. IEEE T Antenn Propag 2011; 59: 4329-4333.

[10] Kumar C, Guha D. Nature of cross-polarized radiations from probe-fed circular microstrip antennas and their suppression using different geometries of defected ground structure (DGS). IEEE T Antenn Propag 2012; 60: 92-101.

[11] Thi TN, Van ST, Kwon G, Hwang KC. Single-feed triple band circularly polarized Spidron fractal slot antenna. Prog Electromagn Res 2013; 143: 207-221.

[12] Reddy VV, Sarma NVSN. Triband circularly polarized Koch fractal boundary microstrip antenna. IEEE Antenn Wirel Propag Lett 2014; 13: 1057-60.

[13] Mandal K, Sarkar PP. A compact low profile wideband U-shape antenna with slotted circular ground plane. AEU-Int J Electron C 2016; 70: 336-340.

[14] Kumar R, Kushwala N. Design and investigation of sectoral circular disc monopole fractal antenna and its backscattering. Engineering Science and Technology, an International Journal 2017; 20: 18-27.

[15] Baek JG, Hwang KC. Triple-band unidirectional circularly polarized hexagonal slot antenna with multiple L-shaped slits. IEEE T Antenn Propag 2013; 61: 4831-4835.

[16] Chang TH, Kiang JF. Compact multi-band H-shaped slot antenna. IEEE T Antenn Propag 2013; 61: 4345-4349.

[17] Srivastava K, Kumar R. Study of U-slot electromagnetic band gap structure and its effect on hexagonal patch antenna. In: 2013 Advanced Computing and Communication Technologies Conference; 6–7 April 2013; Rohtak, India. pp. 138-143.

[18] Aissaoui D, Abdelghani LM, Hacen NB, Tayeb A. CPW-fed printed fractal slot antenna for UWB applications. In: IEEE 2016 Antenna Technology and Applied Electromagnetics Conference; 10–13 July 2016; Montreal, Canada. New York, NY, USA: IEEE. pp. 1-2.

[19] Saidatul NA, Azremi AAH, Soh PJ. A hexagonal fractal antenna for multiband application. In: IEEE 2007 Intelligent and Advanced Systems Conference; 25–28 November 2007; Malaysia. New York, NY, USA: IEEE. pp. 361-364.

[20] Samreen KS, Chaudhary R. Miniaturized hexagonal-shaped fractal slot microstrip antenna For WLAN application using DGS. In: Springer 2013 Advances in Communication and Control Systems Conference; 18–19 January 2013; Mumbai, India. Berlin, Germany: Springer. pp. 388-392.

[21] Upadhyay D, Acharya I, Gupta A. DGS & DMS based hexagonal fractal antenna for UWB applications. In: IEEE 2015 Communications and Signal Processing Conference; 2–4 April 2015; Tamil Nadu, India. New York, NY, USA: IEEE. pp. 176-179.

[22] Tripathi S, Akhilesh M, Yadav S. Hexagonal fractal ultra-wideband antenna using Koch geometry with bandwidth enhancement. IET Microw Anten P 2014; 8: 1445-1450.

[23] Li D, Mao JF. Coplanar waveguide-fed Koch-like sided Sierpinski hexagonal carpet multifractal monopole antenna. IET Microw Anten P 2014; 8: 358-366.

[24] Aissaoui D, Hacen NB, Denidni AT. UWB hexagonal monopole fractal antenna with additional trapezoidal elements. In: IEEE 2015 Ubiquitous Wireless Broadband Conference; 4–7 October 2015; Canada. New York, NY, USA: IEEE. pp. 1-4.

[25] Vummadisetty PN, Kumar R. Design of compact octagonal slotted hexagonal and rectangular shaped monopole antennas for dual/UWB applications. Turk J Elect Eng & Comp Sci 2016; 24: 2806-2824.

[26] Kumar R, Naidu PV, Kamble V. Design of asymmetric slot antenna with meandered narrow rectangular slit for dual band applications. Prog Electromagn Res B 2014; 60: 111-123.

[27] Wu MT, Chuang ML. Multi broadband slotted bow-tie monopole antenna. IEEE Antenn Wirel Propag Lett 2015; 14: 887-890.

[28] Guterman J, Moreira AA, Peixeiro C. Microstrip fractal antennas for multistandard terminals. IEEE Antenn Wirel Propag Lett 2004; 3: 351-355.

[29] Mahatthanajatuphat C, Saleekaw S, Akkaraekthalin P. A rhombic patch monopole antenna with modified Minkowski fractal geometry for UMTS, WLAN, and mobile WIMAX application. Prog Electromagn Res 2009; 89: 57-74.

[30] Khan OM, Islam ZU, Rashid I, Bhatti FA, Islam QU. Novel miniaturized Koch pentagonal fractal antenna for multiband wireless applications. Prog Electromagn Res 2013; 141: 693-710.

[31] Mahatthanajatuphat C, Akkaraekthalin P. A bidirectional multiband antenna with modified fractal slot fed By CPW. Progress Electromagn Res 2009; 95: 59-72.